

CMB-S4 Simulation of Bias in r

Author:

William Aedhan Cornish Scott

Capstone Advisor:

Dr. Colin Bischoff

Physics Department
University of Cincinnati

April 2024

1 Introduction

The quest to understand the early universe has led cosmologists to research the Cosmic Microwave Background (CMB) with increasing accuracy and scrutiny. The CMB, the residual thermal radiation from the Big Bang comes encoded with polarization signatures such as B-modes, which offer a unique window of understanding into the inflationary epoch, an era of rapid expansion believed to have occurred within fractions of a second after the Big Bang. The detection and analysis of B-mode polarization patterns are important as they provide direct evidence of inflationary gravitational waves, ripples in the fabric of spacetime generated during this time of inflation. These gravitational waves have in theory imprinted a distinct pattern in the CMB polarization, distinguishing B-modes from the more commonly observed E-modes that arise primarily from density fluctuations.

The CMB-S4 experiment represents a monumental step forward in this investigation. It aims not only to detect these B-modes but also to measure the ratio of the power spectrum of tensor perturbations to the power spectrum of scalar perturbations at a given scale. This ratio, a critical parameter known as r will help delineate the relative strength of inflationary gravitational waves to density perturbations, refining our understanding of inflation and restricting the plethora of inflationary models.

Depending on the outcome of the experiment, CMB-S4 has set divergent goals. In the absence of B-Mode detection, it aims to establish a 2 sigma limit at 10^{-3} while a detection scenario targets measuring r at $3 * 10^{-3}$ with 5 sigma certainty. Simulations underpin these objectives, with a 1 sigma statistical error on R of $5 * 10^{-4}$ identified as sufficient sensitivity for determining detection feasibility. The experiment will feature an array of telescopes including three small aperture telescopes (SATs) at the South Pole, a 5 meter large aperture telescope for de-lensing, and two 6-meter telescopes in Chile focusing on non-inflation science, with a target first light in 2032.

2 Bandpass Systematics for CMB-S4 small aperture telescopes

Central to making meaningful measurements of the CMB is the challenge of distinguishing the signal from foreground contaminants- primarily thermal emissions from dust and synchrotron emissions both from the Milky Way. These foregrounds introduce noise into our sky maps, complicating the observation of the CMB's features. CMB-S4's strategy involves multifrequency measurements across eight frequency bands spanning an order of magnitude in frequency. The bands are 26, 40, 85, 95, 145, 155, 230, and 280 GHz. With maps at 8 frequencies, there are a variety of analysis methods to remove the foreground, here we have used the

BICEP method. This method necessitates accurate knowledge of bandpasses- the range of frequencies each detector is sensitive to, as errors here can introduce significant biases in our measurements of r .

Foreground modeling is vital, requiring the combination of CMB signals with foreground components, informed by multifrequency data to constrain the parameters of both. The spectra of these foregrounds vary distinctly, with synchrotron emissions following a power law that intensifies at lower frequencies due to the galaxy's magnetic fields influencing electron paths, and dust emissions resembling a modified blackbody radiation pattern, compounded by a power law representing dust emissivity frequencies. Understanding these spectra and their representation in our observations is crucial for effective foreground cleaning.

For this project, I will explore the effects of mis-modeling these foregrounds by manipulating band-pass parameters, aiming to uncover potential biases in our measurement of r . This investigation extends beyond previous map-level analyses by examining the model at the wafer level, which should offer new insights into the challenges and potential solutions towards this piece of CMB-S4's science goal.

3 Simulations of CMB-S4 per wafer scan description

Each CMB-S4 instrument will have a multitude of wafers sensitive to a specific frequency of signal. In order to simulate the the variations between individual wafers, we need to run a scan simulation for each wafer individually. We do this by taking the focalplane maps from the `s4sim` repository, and isolating individual wafers within these arrays. The 85GHz array and an individual wafer in the array are shown in figures 1 and 2.

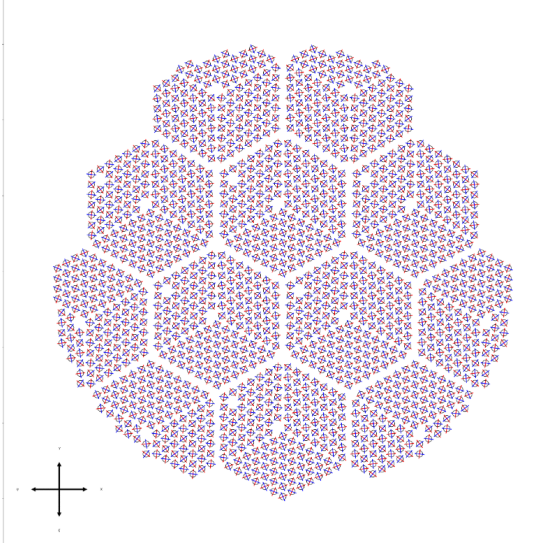


Figure 1: Full 85GHz Array

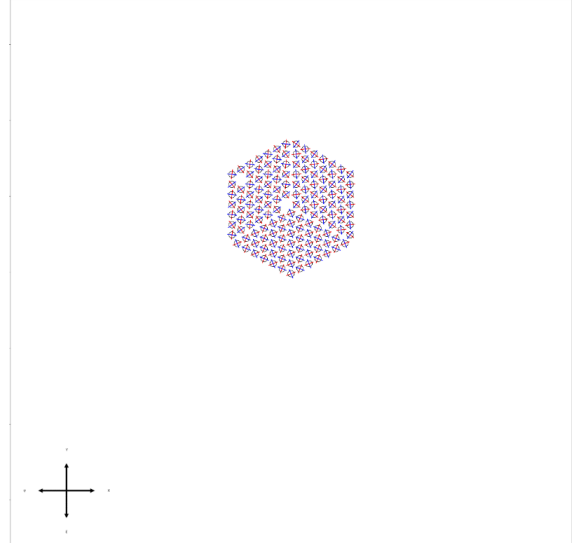


Figure 2: Individual Wafer from 85GHz Array

Each of these wafers is assigned an observation schedule that delineates celestial coordinates and durations for its scans. Our schedule adopts an azimuthal scanning strategy, which avoids changes in elevation during the observation to mitigate the fluctuations in atmospheric signal that changes in elevation would induce. As our instruments are at the south pole, scanning in an azimuthal direction is equivalent to right ascension scanning, ensuring a constant atmospheric depth across observations. The schedule used is 3.5 days out of the 10 year experiment, but the schedule is highly redundant so we cover all the same area in that shortened time and adjust the noise model later to account for the difference between the simulation and what would be the noise level present in the real experiment after 10 years.

#Site	Telescope	Latitude [deg]	Longitude [deg]	Elevation [m]	Az min	Az max	El	Pass	Sub
SOUTH_POLE	SAT	-89.991	-44.650	2843.0					
#	Start time UTC	Stop time UTC	Rotation	Patch name					
2027-04-01	00:00:00	2027-04-01 01:24:00	225.00	POLE_DEEP	210.00	280.67	52.36	0	0
2027-04-01	01:30:00	2027-04-01 02:54:00	225.00	POLE_DEEP	187.44	258.11	52.61	0	1
2027-04-01	03:00:00	2027-04-01 04:24:00	225.00	POLE_DEEP	164.88	235.55	52.86	0	2
2027-04-01	04:30:00	2027-04-01 05:54:00	225.00	POLE_DEEP	142.32	212.99	53.11	0	3
2027-04-01	06:00:00	2027-04-01 07:24:00	225.00	POLE_DEEP	119.77	190.44	53.36	0	4
2027-04-01	07:30:00	2027-04-01 08:54:00	225.00	POLE_DEEP	97.20	167.88	53.61	0	5
2027-04-01	09:00:00	2027-04-01 10:24:00	225.00	POLE_DEEP	74.64	145.32	53.86	0	6
2027-04-01	10:30:00	2027-04-01 11:54:00	225.00	POLE_DEEP	52.08	122.75	54.11	0	7
2027-04-01	12:00:00	2027-04-01 13:24:00	225.00	POLE_DEEP	29.51	100.19	54.36	0	8
2027-04-01	13:30:00	2027-04-01 14:54:00	225.00	POLE_DEEP	6.95	77.63	54.61	0	9
2027-04-01	15:00:00	2027-04-01 16:24:00	225.00	POLE_DEEP	344.38	415.07	54.86	0	10
2027-04-02	09:00:00	2027-04-02 10:24:00	270.00	POLE_DEEP	73.66	144.34	52.36	2	0
2027-04-02	10:30:00	2027-04-02 11:54:00	270.00	POLE_DEEP	51.09	121.78	52.61	2	1
2027-04-02	12:00:00	2027-04-02 13:24:00	270.00	POLE_DEEP	28.53	99.22	52.86	2	2
2027-04-02	13:30:00	2027-04-02 14:54:00	270.00	POLE_DEEP	5.96	76.66	53.11	2	3
2027-04-02	15:00:00	2027-04-02 16:24:00	270.00	POLE_DEEP	343.40	414.09	53.36	2	4
2027-04-02	16:30:00	2027-04-02 17:54:00	270.00	POLE_DEEP	320.83	391.52	53.61	2	5
2027-04-02	18:00:00	2027-04-02 19:24:00	270.00	POLE_DEEP	298.26	368.96	53.86	2	6
2027-04-02	19:30:00	2027-04-02 20:54:00	270.00	POLE_DEEP	275.70	346.38	54.11	2	7
2027-04-02	21:00:00	2027-04-02 22:24:00	270.00	POLE_DEEP	253.14	323.82	54.36	2	8
2027-04-02	22:30:00	2027-04-02 23:54:00	270.00	POLE_DEEP	230.58	301.25	54.61	2	9
2027-04-03	00:00:00	2027-04-03 01:24:00	270.00	POLE DEEP	208.02	278.69	54.86	2	10

Figure 3: 2 Days of scan schedule used on wafers for scan simulation

Taking our scan schedule and our wafer information, we then use Time Ordered Astrophysics Scalable Tools (TOAST) default noise model and apply it to a generic sky map. Using TOAST we are able to simulate the wafer observing this noisy sky map with our scan schedule, which allows us to generate an inverse covariance map which shows how long a given wafer spent observing a given position on the sky. This is done for every wafer in each detector for frequencies of 30GHz, 85GHz, 95GHz, and 220GHz. Figure 4 shows an inverse covariance map generated by the wafer in figure 2 and the scan schedule in figure 3.

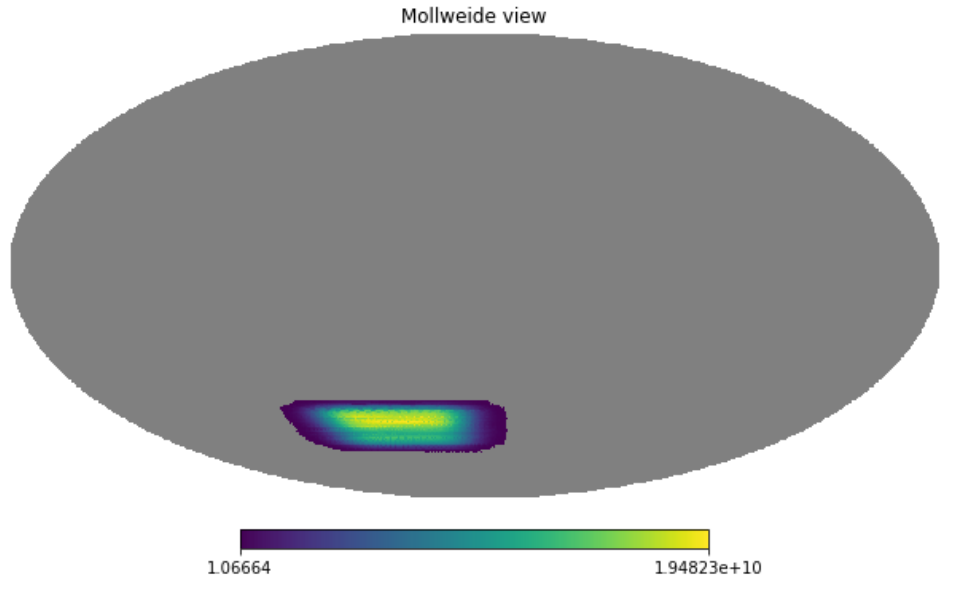


Figure 4: Inverse covariance map of single 85GHz wafer following scan schedule: units are in inverse microKelvin

We can see in figure four that a single wafer spends a lot more time observing some areas of the sky than others with our scan strategy. It also has significant breaks in its observing area. Figure 5 shows another wafer selected from the 85 GHz array, further demonstrating the differences in what sky area the detector covers.

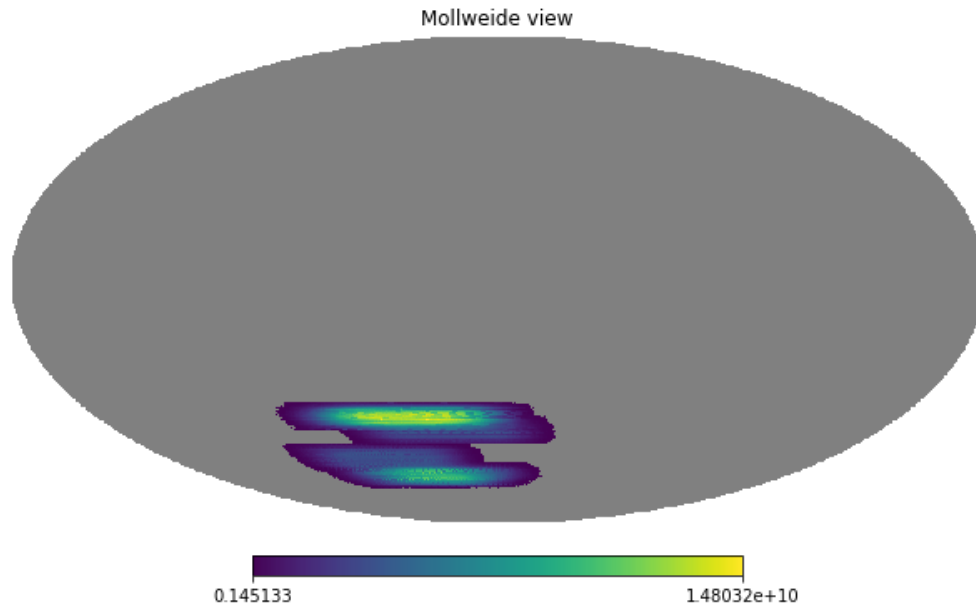


Figure 5: Inverse covariance map of single 85GHz wafer following scan schedule: units are in inverse microKelvin

Having many wafers working together gets us a more reasonably covered sky, and looks more like figure 6.

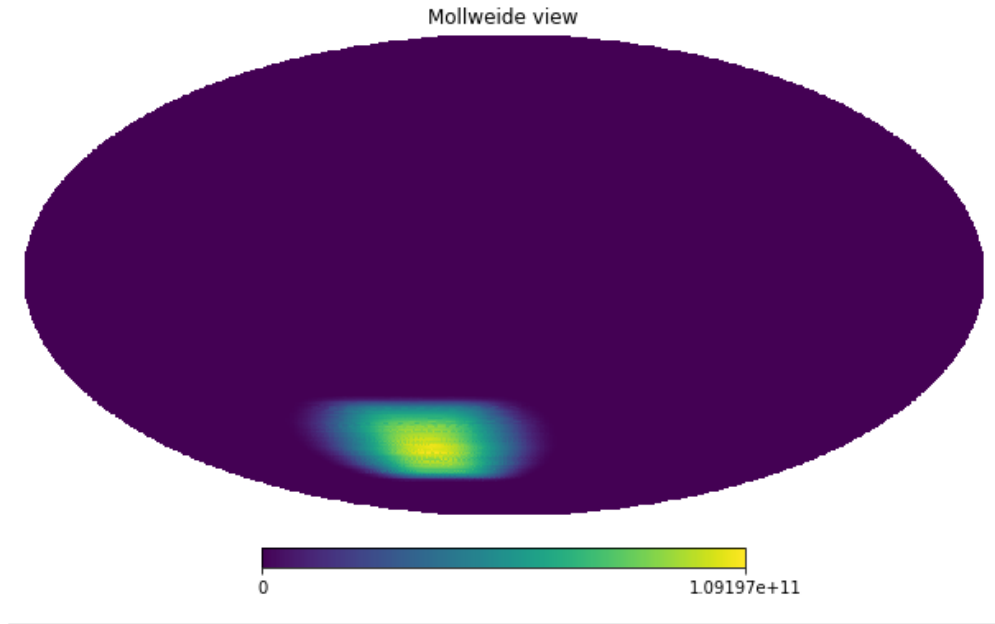


Figure 6: Inverse covariance map of full 85GHz detector following scan schedule: units are in inverse microKelvin

As would be expected we see the closer to the center of the observing area has higher inverse covariance values, indicating that more time was spent observing there.

4 Simulated Maps with Bandpass systematics

There are multiple pieces to the puzzle of a fully simulated map. Having fully covered the TOAST simulation in the previous section, we move onto the rest of it. The simulation process begins with generating CMB temperature and Q,U stokes parameter polarization maps of the full sky. We use a multitude of 'telescope models' to determine what these will look like. Figures 7 and 8 show Q and U polarization maps for our LF-1 parameters

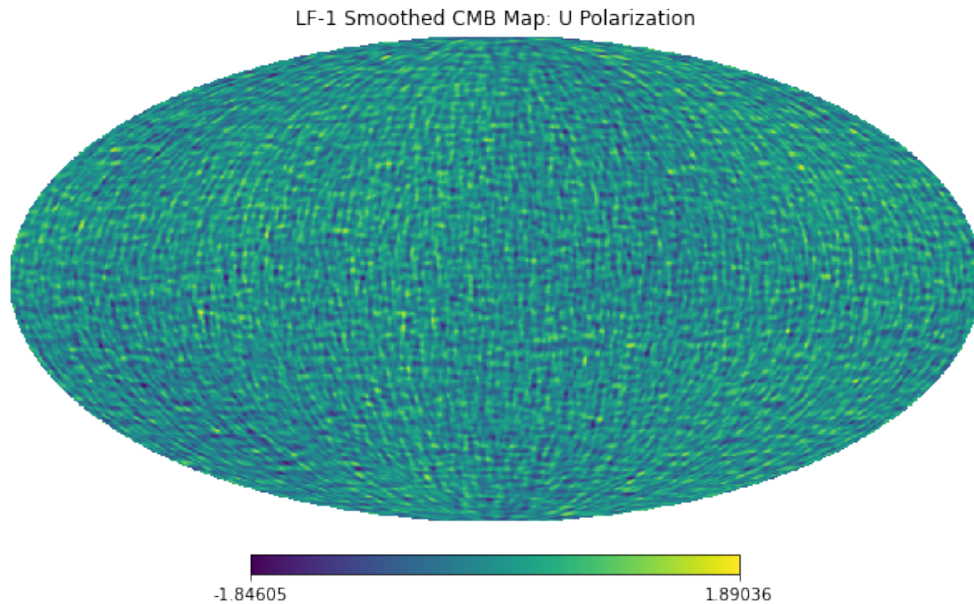


Figure 7: Full Sky Q Polarization Map: units are in microKelvin

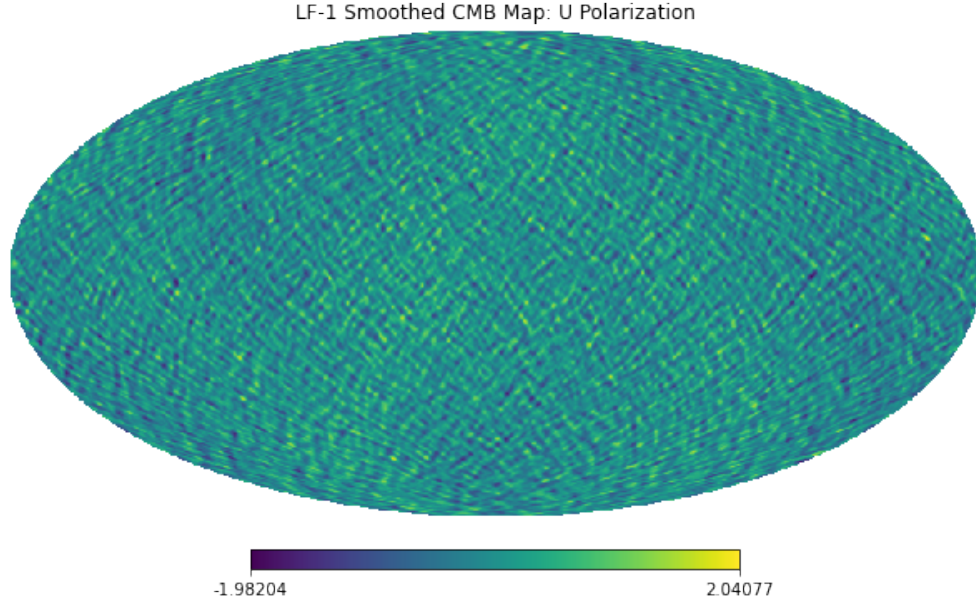


Figure 8: Full Sky U Polarization Map: units are in microKelvin

We then create separate noise maps for the temperature map and the two polarization maps for each set of telescope parameters. The noise model is based on a power spectrum C_l (equation 1) which is defined for each multipole moment l . The formula used incorporates a knee frequency and a power law exponent, which are characteristic of $1/f$ noise models often used in CMB science. The noise maps are shown in figures 9 and 10

$$C_l^{\text{noise}(i)} = A \left(1 + \left(\frac{l}{l_{\text{knee}}} \right)^\alpha \right) \quad (1)$$

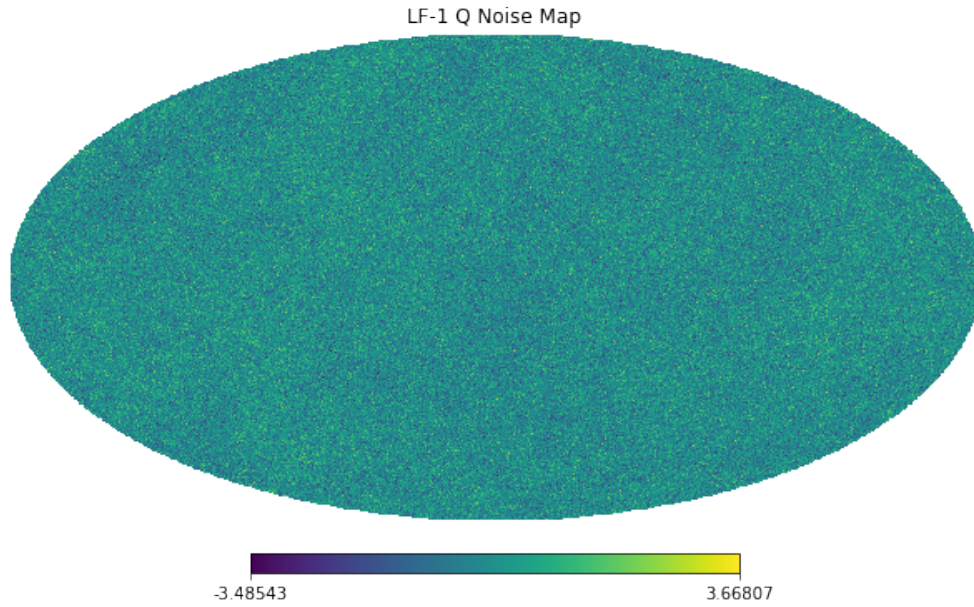


Figure 9: Full Sky Q Polarization Noise Map: units are in microKelvin

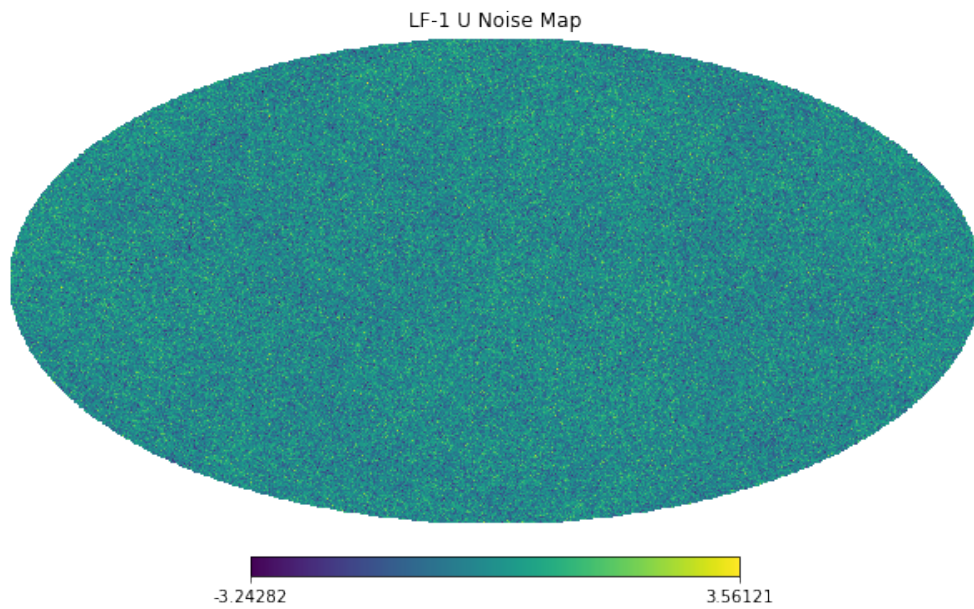


Figure 10: Full Sky U Polarization Noise Map: units are in microKelvin

Using the full sky noise maps with the observation areas from the TOAST simulation, we generate our fully adjusted noise maps shown in figure 11 to use for the final simulation.

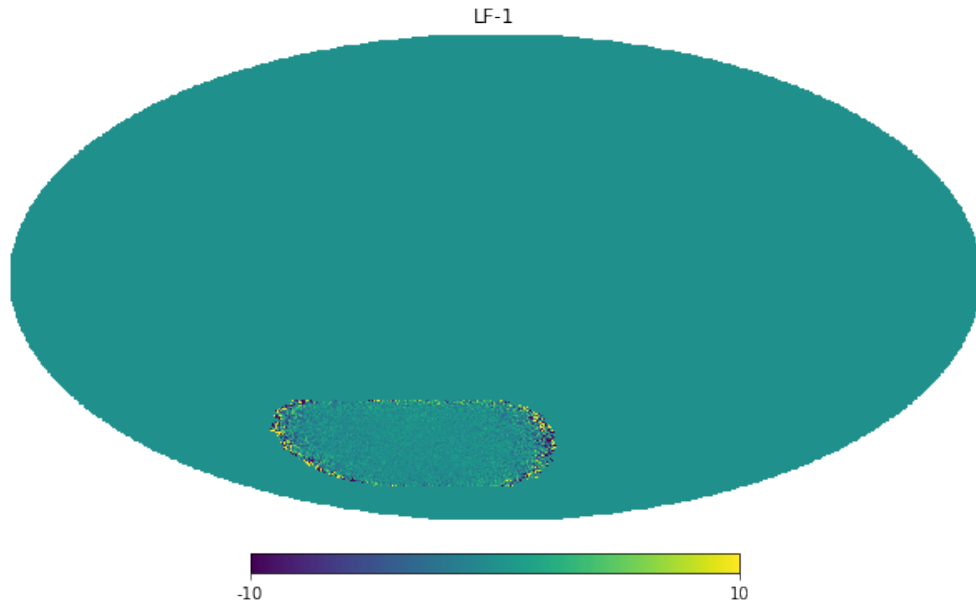


Figure 11: LF-1 Parameter Fully Adjusted Noise Map

Taking these fully adjusted noise maps and summing them with the corresponding smoothed CMB maps takes us to figures 12 and 13

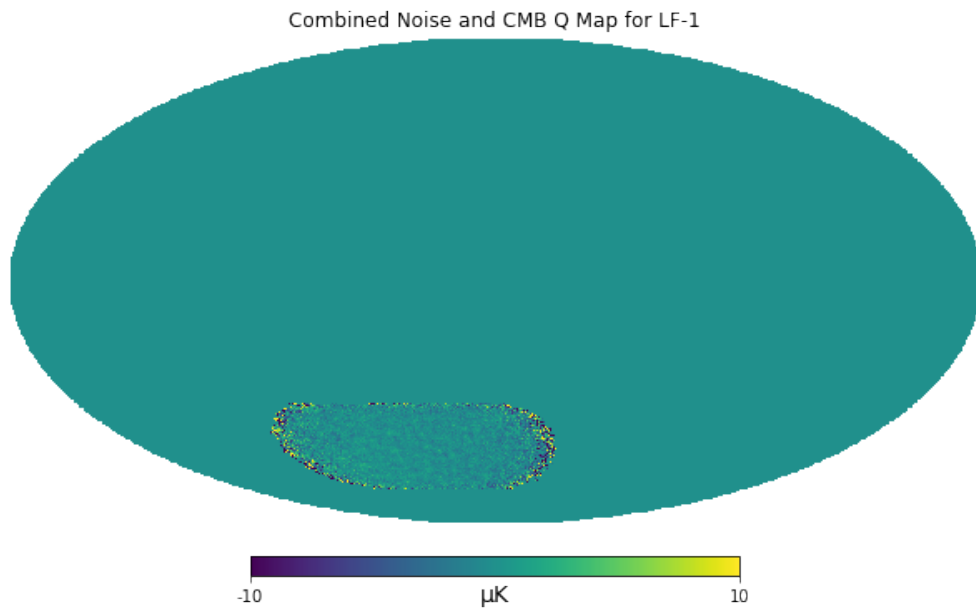


Figure 12: Linear combination of All noise and Smoothed CMB Q map

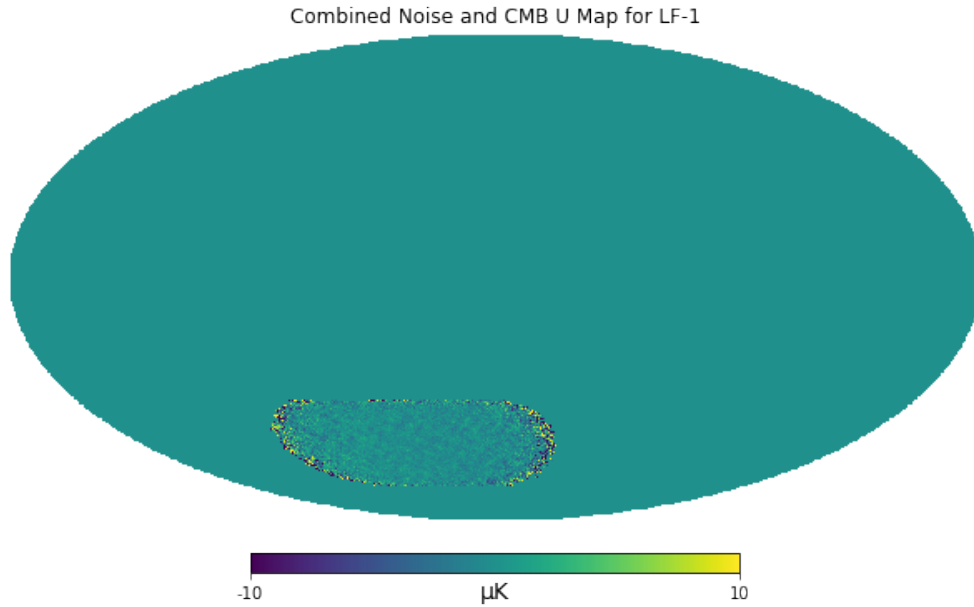


Figure 13: Linear combination of All noise and Smoothed CMB U map

The final piece missing from our full simulations are the foregrounds. We generate foreground models with the `pysm3` package in Python. We generate foreground maps for each individual wafer within a given frequency's focal plane, include slight fluctuations to simulate wafer to wafer variations, and then recombine those foreground maps to get the full foreground map for the observation. Figures 14-16 show an example foreground Q map for the 30GHz array with LF-1 telescope parameters. Figure 14 shows the map without wafer variation, Figure 15 shows with variation, and 16 is the difference map between the two.

Summed Foreground Q Map without Systematics (uK_CMB)

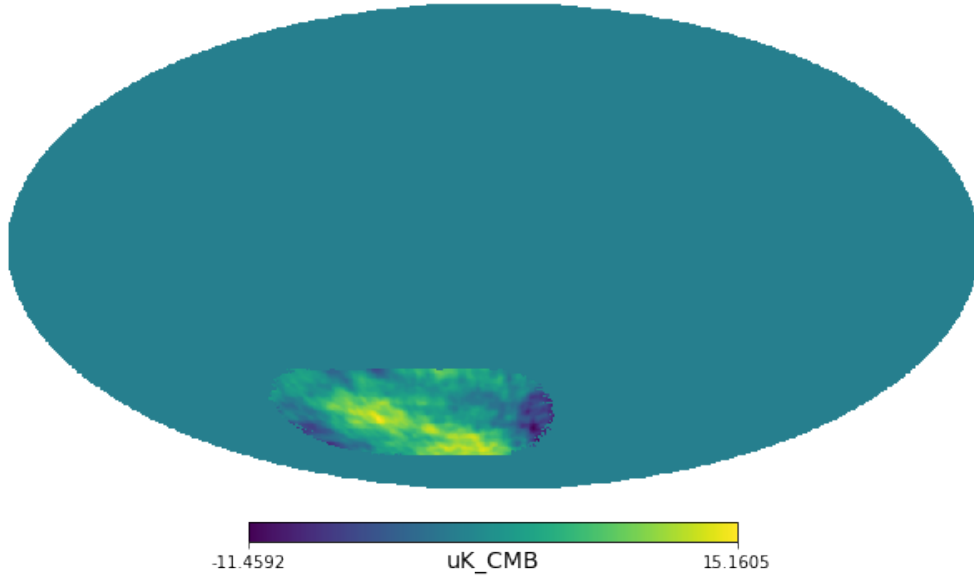


Figure 14: Foreground Q map without wafer systematic: no statistical variation between individual wafer foreground sims

Summed Foreground Q Map with Systematics (uK_CMB)

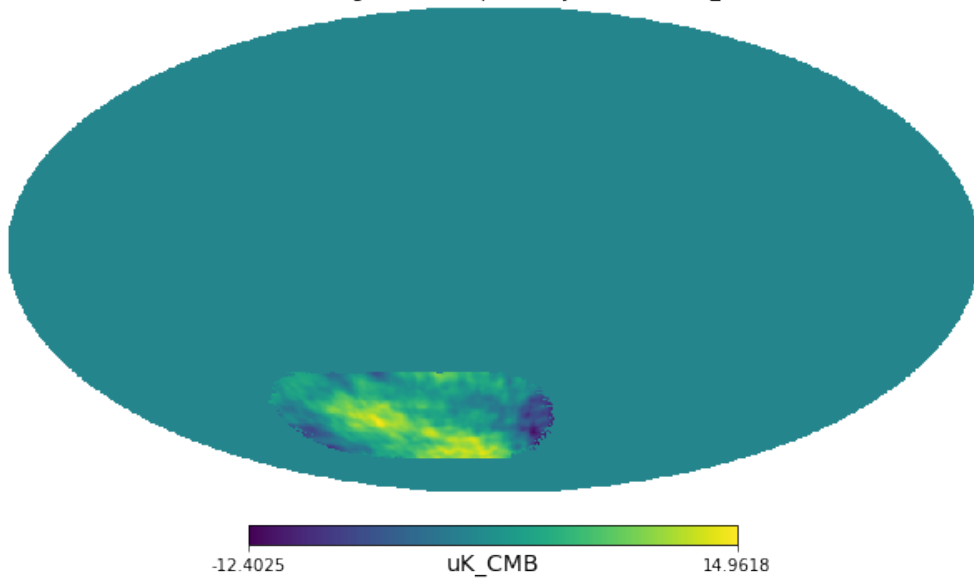


Figure 15: Foreground Q map with wafer systematic: 1 percent statistical variation between individual wafer foreground sims

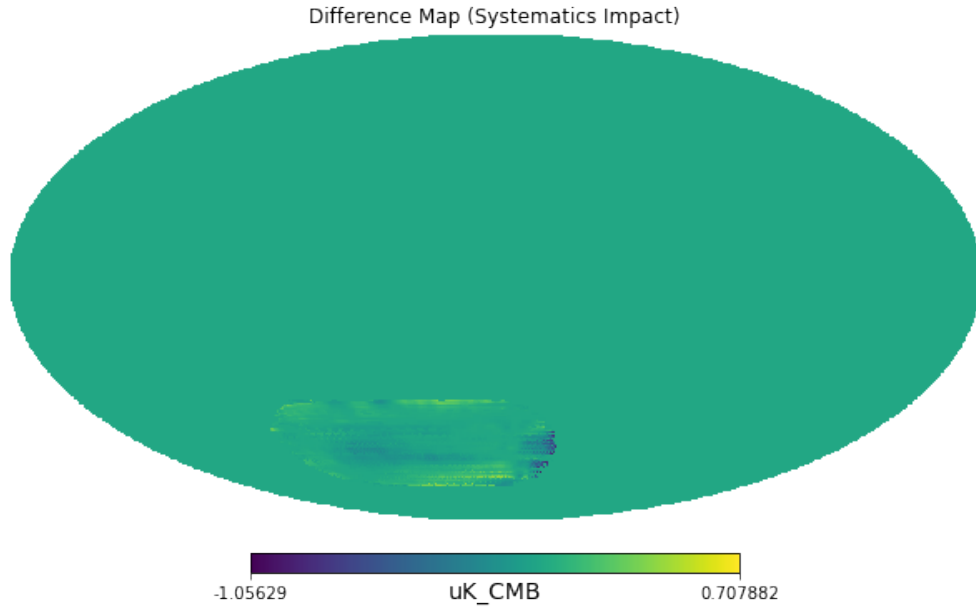


Figure 16: Difference Map to show effect of wafer variation in foregrounds

We sum the foreground maps with the combined Noise and CMB maps for the polarization maps, to arrive at our final result, a choice selection of which is shown in figures 17 and 18

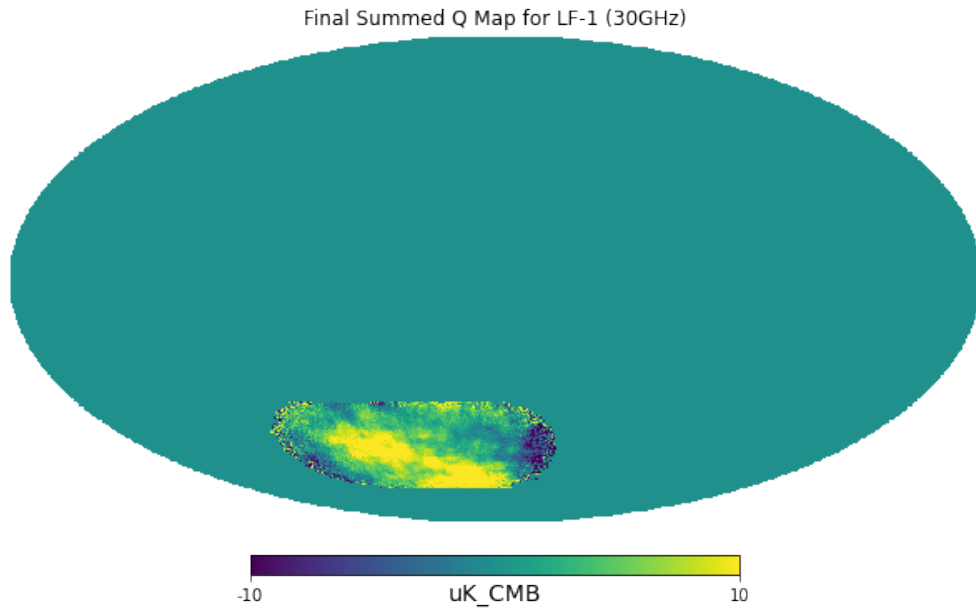


Figure 17: Fully simulated observation of Q map with wafer systematics

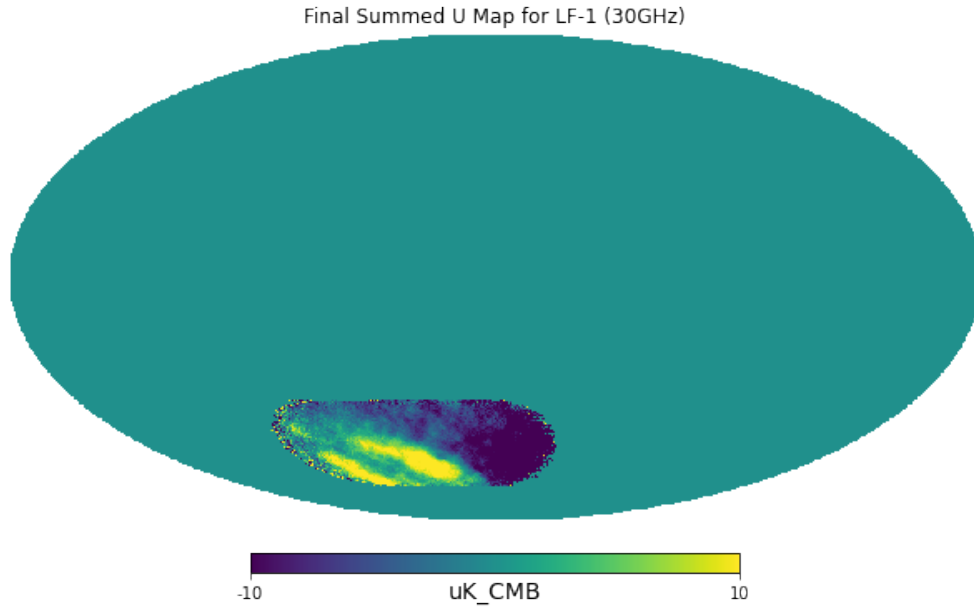


Figure 18: Fully simulated observation of U map with wafer systematics

These full maps combine beam-smoothed cmb polarization signal, a noise signal following equation 1, wafer-varied foreground noise, and these maps instead of being full sky, are only built off the portions that a real telescope would observe while following a CMB-S4 observation schedule. These maps will be the foundation on which further research can be conducted into determining bias in the aforementioned tensor to scalar ratio 'r', and other questions which can be answered with a robust pipeline for generating such simulations.

References

- [1] Kamionkowski, M., & Kovetz, E. D. (2015). The Quest for B Modes from Inflationary Gravitational Waves. *arXiv:1510.06042 [astro-ph.CO]*. Available at: <https://doi.org/10.48550/arXiv.1510.06042>
- [2] Abazajian, K., Addison, G., Adshead, P., Ahmed, Z., Allen, S. W., Alonso, D., Alvarez, M., Anderson, A., Arnold, K. S., Baccigalupi, C., et al. (2019). CMB-S4 Science Case, Reference Design, and Project Plan. *arXiv:1907.04473 [astro-ph.IM]*. Available at: <https://doi.org/10.48550/arXiv.1907.04473>
- [3] Abazajian, K. N., Adshead, P., Ahmed, Z., Allen, S. W., Alonso, D., Arnold, K. S., Baccigalupi, C., Bartlett, J. G., Battaglia, N., Benson, B. A., et al. (2016). CMB-S4 Science Book, First Edition. *arXiv:1610.02743 [astro-ph.CO]*. Available at: <https://doi.org/10.48550/arXiv.1610.02743>
- [4] Abazajian, K., Abdulghafour, A., Addison, G. E., Adshead, P., Ahmed, Z., Ajello, M., Akerib, D., Allen, S. W., Alonso, D., Alvarez, M., et al. (2022). Snowmass 2021 CMB-S4 White Paper. *arXiv:2203.08024 [astro-ph.CO]*. Available at: <https://doi.org/10.48550/arXiv.2203.08024>
- [5] Planck Collaboration, Akrami, Y., Ashdown, M., Aumont, J., Baccigalupi, C., Ballardini, M., Banday, A. J., Barreiro, R. B., Bartolo, N., Basak, S., et al. (2020). Planck 2018 results. XI. Polarized dust foregrounds. *Astronomy & Astrophysics*, *641*, A11. <https://doi.org/10.1051/0004-6361/201832618>
- [6] Choi, S. K., & Page, L. A. (2015). Polarized galactic synchrotron and dust emission and their correlation. *Journal of Cosmology and Astroparticle Physics*, *2015*(12), 020. <https://doi.org/10.1088/1475-7516/2015/12/020>
- [7] Keck Array, BICEP2 Collaborations: Ade, P. A. R., Ahmed, Z., Aikin, R. W., Alexander, K. D., Barkats, D., Benton, S. J., Bischoff, C. A., Bock, J. J., Bowens-Rubin, R., Brevik, J. A., et al. (2018). Constraints on Primordial Gravitational Waves using Planck, WMAP, and New BICEP2/Keck Observations through the 2015 Season. *Physical Review Letters*, *121*(22), 221301. <https://doi.org/10.1103/PhysRevLett.121.221301>
- [8] CMB-S4 Collaboration: Abazajian, K., Addison, G. E., Adshead, P., Ahmed, Z., Akerib, D., Ali, A., Allen, S. W., Alonso, D., Alvarez, M., Amin, M. A., et al. (2020). Forecasting Constraints on Primordial Gravitational Waves. *Astrophysical Journal*. <https://doi.org/10.3847/1538-4357/ac1596>

- [9] Kisner, T., Keskitalo, R., Zonca, A., Madsen, J. R., Savarit, J., Tomasi, M., Cheung, K., Puglisi, G., Liu, D., & Hasselfield, M. (2021). `hpc4cmb/toast`: Update Pybind11 (2.3.14). Zenodo. <https://doi.org/10.5281/zenodo.5559597>
- [10] CMB-S4 Collaboration. (2021). *s4sim: Simulation tools for the CMB-S4 project*. Available at: <https://github.com/CMB-S4/s4sim>
- [11] Thorne, B., Dunkley, J., Alonso, D., & Naess, S. (2016). The Python Sky Model: software for simulating the Galactic microwave sky. *arXiv:1608.02841 [astro-ph.CO]*. <https://doi.org/10.1093/mnras/stx949>